Cross sections for electron scattering from thiophene for a broad energy range

Cross sections for electron scattering from thiophene for a broad energy range

Alexandra Loupas,[1, a)] Ana. I. Lozano,[2] Francisco Blanco,[3] Jimena D. Gorfinkiel,[4, b)] and Gustavo García[2]

[1)] *Laboratório de Colisões Atómicas e Moleculares, CEFITEC, Departamento de Física, Faculdade de Ciências e Tecnologia, Universidade Nova de Lisboa, Campus de Caparica, 2829-516, Portugal*

[2)] *Instituto de Física Fundamental, Consejo Superior de Investigaciones Científicas, Serrano 113-bis, 28006 Madrid, Spain*

[3)] *Departamento de Física Atómica, Molecular y Nuclear, Universidad Complutense de Madrid, Ciudad Universitaria, 28040 Madrid.*

[4)] *School of Physical Sciences, The Open University, Walton Hall, Milton Keynes, MK7 6AA, United Kingdom.*

(Dated: 26 June 2018)

We present cross sections for elastic and inelastic electron scattering from thiophene calculated in the energy range 0.1-1000 eV. The R-matrix and IAM-SCAR methods were used for low-energy and intermediate and high scattering energies, respectively. The results provide a consistent picture of the scattering process in the whole energy range. The effect of including an interference term in the IAM-SCAR approach is considered. Agreement with prior theoretical results is also discussed.

PACS numbers: 34.80-i,34.80.Bm,34.80.Gs
Keywords: electron scattering, cross sections

[a)] School of Physical Sciences, The Open University, Walton Hall, Milton Keynes, MK7 6AA, United Kingdom

[b)] Electronic mail: Jimena.Gorfinkiel@open.ac.uk

I. INTRODUCTION

Understanding and characterizing electron scattering from molecules has received increasing attention from the scientific community over the last couple of decades. One of the main reasons is the importance of these scattering phenomena in a number of applied fields.[1] In addition, experimental and software developments as well increased computational resources have made it possible to determine cross sections for more complex targets, more processes and more accurately.

The modelling of a number of physical phenomena requires the availability of cross sections for all possible electron-induced processes (elastic scattering, target excitation, dissociative electron attachment (DEA), ionization, neutral and dipolar dissociation, etc.) for a broad energy range. For example, Monte Carlo simulations of track structures to model radiation induced damage in DNA, in which the interaction history of the incident and released particles is followed step-by-step until their energy falls below a specified threshold[2], requires knowledge of a large number of cross sections. Modelling of plasmas[3] and transport processes of charged particles in gases to obtain electron densities, average velocities, etc.[4] also require cross section data as input.

The main focus of recent scattering studies has been biological molecules. The research has been stimulated, among other works, by the study of Boudaïffa *et al.*[5] that showed that electrons with sub-ionization energies were able to induce single and double strand breaks in DNA, through the DEA process. Extensive work has been performed to understand resonance formation and DEA of DNA constituents and other biomolecules[6,7]. Somewhat scarcer is work to obtain cross sections for the various processes of interest: experimentally, it can be hard to determine absolute cross section for a number of reasons[7]; theoretically, the characteristics of the molecules (electron-rich, with many low-lying electronic states, big dipole moments and low symmetry) also make it more difficult to calculate accurate data.

Other targets studied have been molecules that can be seen as models of the building blocks of DNA, proteins, etc., and that either have higher symmetry (and are thus easier to study theoretically) or from which sufficient gas pressure can be more easily achieved (and experiments are more easily carried out). Among these molecules are, for example, tetrahydrofuran[8–12] (used as a model for deoxyribose), the first biological target for which electronic excitation cross sections were calculated and pyrimidine, that can be seen as a

model for the pyrimidic nucleobases[13,14]. More recently, attention has turned to aminoacids and other biomolecules.[7]

This work focuses on low energy electron collisions with thiophene (C_4H_4S), one of the most used units in anti-inflammatory drugs[15]. Thiophene is a prototypical, fully conjugated, heterocyclic molecule which contains one heavy and highly polarizable sulphur atom. Electron scattering from thiophene has been studied both theoretically[16–19] and experimentally[20–23]. Most of these works focus on resonance formation and DEA. da Costa *et al.*[17], used the Schwinger multichannel method with pseudopotentials (SMCPP) in the energy range of 0.5-6 eV and reported integral and differential elastic as well as momentum transfer cross sections; the main focus of their work were the low-lying π^* and σ^* resonances. Mozejko *et al.*[16] calculated integral elastic and ionization cross sections at intermediate and high electron-impact energies using the additivity rule[24,25] and the binary-encounter-Bethe approach: the total elastic cross sections is calculated from the same cross sections for the constituent atoms of the target molecule. In addition, Vinodkumar *et al*[18] presented cross sections determined with the R-matrix method; however, their calculations suffer from a number of problems discussed elsewhere[19].

Here, as we have done in the past for other targets (pyrazine[26], pyrimidine[27] and pyridine[28]), we present integral and differential elastic and integral inelastic cross sections for a broad range of energies, calculated using the R-matrix[29] and IAM-SCAR[30] methods at low, and intermediate and high energies respectively. The use of both methods provides a consistent picture of the scattering process in the whole energy range.

II. IAM-SCAR METHOD

The IAM-SCAR method is based on an independent atom representation (IAM) complemented with a screening-corrected additivity rule (SCAR) and it has already been extensively employed to calculate electron-scattering cross sections for a wide variety of molecular targets (see Sieradzka *et al.*[28] and references therein), over a broad energy range (0.1-1000 eV).

The calculation method has been explained in detail in previous publications so we will omit its description. However, we have recently incorporated some interference terms to the calculation of the molecular scattering amplitudes[31] which are relevant for this study. We

will briefly summarize this development here. The molecular scattering amplitude is derived from the common expression for multicentre dispersion:

$$F(\theta) = \sum_{\text{atoms}} f_i(\theta) e^{i\mathbf{q}\cdot\mathbf{r}_i} \tag{1}$$

Here, $\mathbf{q} = \mathbf{k}_{out} - \mathbf{k}_{in}$ is the momentum transfer, $\mathbf{r}_i$ is the position of atom i and $f_i(\theta)$ the corresponding atomic scattering amplitude, with θ the electron scattering angle. By averaging its squared modulus, $|F(\theta)|^2$, for all the molecular orientations, the differential elastic cross sections are derived according to:

$$\begin{aligned}
\frac{d\sigma^{\text{elastic}}_{\text{molec}}}{d\Omega} &= \sum_{i,j} f_i(\theta) f_j^*(\theta) \frac{\sin qr_{ij}}{qr_{ij}} \\
&= \sum_i |f_i(\theta)|^2 + \sum_{i\neq j} f_i(\theta) f_j^*(\theta) \frac{\sin qr_{ij}}{qr_{ij}} \\
&= \sum_i \frac{d\sigma^{\text{elastic}}_{\text{atom}_i}}{d\Omega} + \frac{d\sigma}{d\Omega}^{\text{interference}}
\end{aligned} \tag{2}$$

where $q = |\mathbf{q}| = 2k\sin(\theta/2)$, r_{ij} is the distance between atoms i and j, $\sin(qr_{ij})/qr_{ij} = 0$ when $qr_{ij} = 0$, and $\frac{d\sigma}{d\Omega}^{\text{interference}}$ represents the $\sum_{i\neq j}$ interference contribution to the molecular differential cross section. By integrating Equation (2), and introducing some screening coefficients (s_i) as described elsewhere[32,33] the integral elastic cross sections are given by:

$$\sigma^{\text{elastic}}_{\text{molec}} = \sum_{\text{atoms}} \sigma^{\text{elastic}}_{\text{atom}_i} + \sigma^{\text{interference}} \tag{3}$$

where $\sigma^{\text{interference}}$ represents the integration of the differential interference contribution. In spite of the oscillatory nature of the interference terms, their main effect is to increase the scattering amplitudes for the smaller angles and therefore their overall contribution to the integral cross sections making it larger. When the interference terms are included in the calculation of the differential and integral molecular cross sections (Equations. (2) and (3)) we refer our IAM-SCAR method as IAM-SCAR+I.

Dipole interactions are not included in the above calculation procedure. However, for molecules with permanent dipole moment, as is the case of thiophene, an independent calculation based on the Born approximation is performed to estimate the averaged rotational

Cross sections for electron scattering from thiophene

excitation cross sections. The method is described in Sierazdka *et al.*[28] and basically considers that the initial rotational state of the target corresponds to the Jth rotational quantum number distribution at 300 K and dipole interactions induce transitions with $\Delta l = \pm 1$. Rotational excitation cross sections are then incoherently added to the corresponding IAM-SCAR values providing the set of data that we will refer to as IAM-SCAR+R (if the interference is not included) and IAM-SCAR+I+R results (when it is).

III. R-MATRIX THEORY

Since the application of the R-matrix method to electron scattering has also been described in great detail elsewhere,[29,34] we only present here a brief summary. All the calculations in this work were performed within the fixed-nuclei approximation using the UKRmol suite.[35]

The basic idea of the R-matrix method is the division of the configuration space into two regions: an inner and an outer region, separated by a sphere of radius a, centered on the center of mass of the system. This sphere must be large enough to contain the charge density of the N-electron target states included in the calculation, as well as that of the orbitals used to build the L^2 functions described below.

In the inner region, correlation and exchange between all the electrons have to be described accurately. The wavefunctions for the $N+1$ electron system can be written as a linear combinations of two types of terms:

$$\Psi_k^{N+1} = \mathcal{A} \sum_{i=1}^{n} \sum_{j=1}^{n_c} \Phi_i(\mathbf{x}_N; \hat{r}_{N+1}; \sigma_{N+1}) \frac{u_{ij}(r_{N+1})}{r_{N+1}} a_{ijk} + \sum_{i=1}^{m} \chi_i(\mathbf{x}_{N+1}) b_{ik} \quad (4)$$

Here $\mathcal{A}$ is the antisymmetrization operator, $\mathbf{x}_N$ and $\mathbf{x}_{N+1}$ stand for the spin *and* space coordinates of all $N/N+1$ electrons, respectively. σ_{N+1} stands for the spin of the scattering electron, and r_{N+1} and $\hat{\mathrm{r}}_{N+1}$ correspond to its radial and angular coordinates respectively. The wave function Φ_i describes the ith electronic state of the N-electron target, as well as the angular and spin behaviour of the scattering electron. The functions $\frac{u_{ij}(r_{N+1})}{r_{N+1}}$ describe

the radial part of the wave function of the scattering electron while the L^2-integrable functions χ_i are crucial for a good description of the short-range polarization-correlation effects. The coefficients a_{ijk} and b_{ik} are determined by the requirement that the functions Ψ_k^{N+1} diagonalize the non-relativistic Hermitian Hamiltonian of the $(N+1)$-electron system.[29]

In the outer region, the problem is much simpler, since exchange and correlation can be neglected. The interaction between the scattering electron and the target molecule is therefore approximated by a single-center multipole potential expansion. The basis functions Ψ_k^{N+1} are used to construct the R-matrix at the boundary between the regions that is then propagated to the asymptotic region, where by matching with known asymptotic expressions, the K-matrix is determined. From the K-matrix one can determine cross sections via the trivally obtained T-matrices as well as extract resonance parameters (i.e. position and width).

The choice of target electronic states and the type of the L^2 functions included in the expansion (4) defines what we call the scattering model. Detailed information about the models and the choice of the appropriate L^2 functions to include can be found elsewhere[29,36]. In this work, we use the Static-Exchange plus Polarization (SEP) and close-coupling (CC) models. At the SEP level, only the target ground state wavefunction is included in expansion (4), so only shape resonances are described well by this method, in which the molecule is allowed to be polarized by the incoming electron. This effect is described by inclusion of the appropriate L^2 configurations: these are built by allowing the scattering electron to occupy one of a set of virtual orbitals (VOs) (i) while the Hartree-Fock configuration describes the ground state or (ii) while single excitations from the ground state configuration are allowed. The choice of how many VOs to include can have a strong effect on the description of resonances, but is less significant for the modelling of cross sections except at very low energies. The SEP model is also able to describe core-excited resonances, although this description is much poorer.

In the more sophisticated Close-Coupling (CC) approximation, a number of target electronic excited states are included in expansion (4). These are normally described at the complete active space (CAS) level and the L^2 functions included are different: here the scattering electron is allowed to occupy either an orbital of the active space or a virtual orbital. Again single excitations from the active space may also need to be included for a good description of polarization effects. Electronic excitation cross sections can be calculated with

this approximation and both shape and core-excited resonances are well described.

In our low-energy calculations, we have used the UKRmol suite to generate K and T-matrices and determine elastic and inelastic integral cross sections. To calculate elastic differential cross sections (DCS), we have used POLYDCS[37]. This program uses a frame-transformation method (see Gianturco and Jain[38] for further information). This is one of several first Born approximation-based "top up" procedures: those partial waves not included in the *ab initio* calculation are incorporated in an approximate way - or, alternatively, we can say that the *ab initio* contribution is a correction of the Born cross section. We note that within the fixed-nuclei approximation, the cross sections for polar targets diverge due the long-range nature of the electron-dipole interaction. The approach used by POLYDCS, that implicitly reintroduces the rotational motion, overcomes this.

A. Details of the calculation

Thiophene, C_4H_4S, is a planar molecule with 44 electrons that belongs to the C_{2v} point group. Its first electronic excitation threshold[20,39–41] is at 3.7 eV and its ionization energy[42] is 8.86 eV. Its dipole moment[43] is 0.52 Debye and its experimentally determined polarizability[44] is 60.8 a_0^3 .

To perform the R-matrix calculations, we have used the molecular geometry described on the NIST website[42], calculated at MP2 level using the cc-pVDZ basis set.

Following our previous work on thiophene[19], we have used the diffuse basis set 6-311G** and Hartree-Fock SCF (HF) and CASSCF orbitals generated with MOLPRO[45] in the SEP and CC calculations respectively. We used a radius a of 15 a_0 and partial waves up to $l = 5$ for the description of the continuum, rather than the more usual $l = 4$. Including the additional $l = 5$ partial wave made negligible difference to the integral elastic cross sections, but it did change somewhat: (i) the shape of the DCS at higher energies for angles above 30°; (ii) the size of the total inelastic cross section for energies above 8 eV. The choice of the model used in the scattering calculation was reported previously[19]; the optimal number of VOs to include was determined to be 35 and 70 at the SEP and CC level, respectively.

Thiophene is an asymmetric top, with rotational constants 3.297×10^{-5}, 2.197×10^{-5} and 1.319×10^{-5} eV. For simplicity, we have treated it as a symmetric top (for which the rotational energies, needed in POLYDCS, can be calculated analytically) using the rotational constants

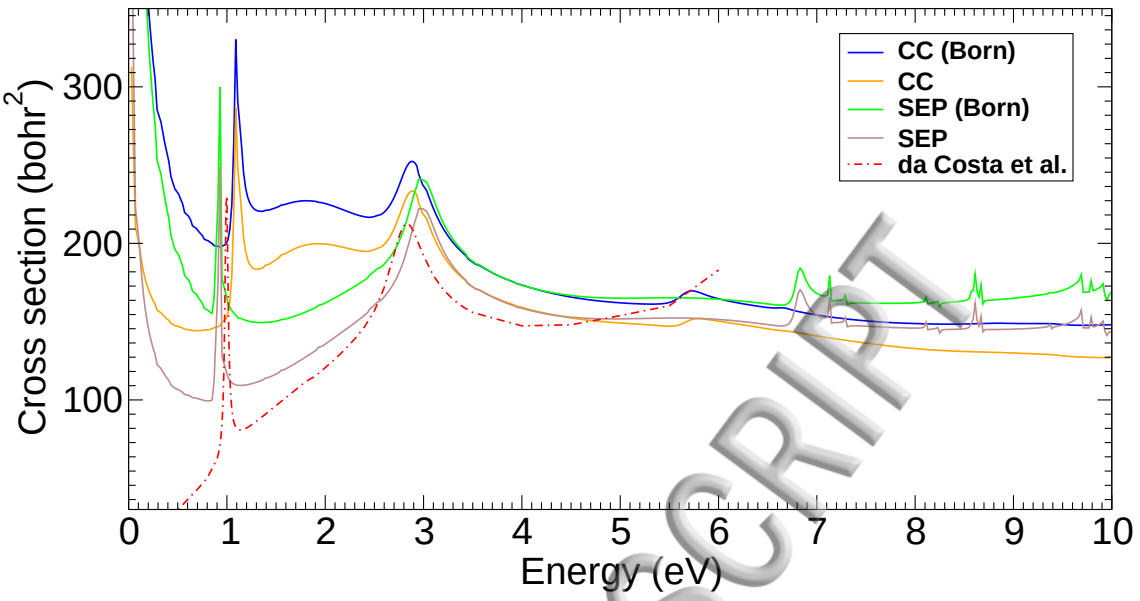

FIG. 1. Integral elastic cross section for electron scattering from thiophene at energies up to 10 eV calculated with the R-matrix approach at SEP and CC levels, with and without the Born correction. Also plotted are the SEP results from da Costa *et al.*[17]

3.297×10^{-5} and 1.758×10^{-5} eV. Tests using other values for the rotational constants led to very similar integral and differential elastic cross sections. The POLYDCS calculations assume the molecule is initially in its ground rotational state and sum over all possible final states with $J < 9$. No inclusion of a Born-type correction for the dipole-allowed excitation processes was attempted, but the effect is not expected to be significant.[19]

IV. RESULTS

In this section we present integral and differential elastic, electronically inelastic and total cross sections in the 0.1-1000 eV energy range. The cross sections calculated using the R-matrix method are most reliable below the ionization threshold; the elastic ones up to $\approx$ 20 eV can be considered to provide reasonable estimate of the actual cross sections. The IAM-SCAR method, conversely, is more accurate at higher energies and is expected to provide poor results in the range where the R-matrix method is most accurate. Our best results could therefore be defined as the R-matrix ones below 10 eV, one of the IAM-SCAR ones above 30 eV and a smooth interpolation between the two in the 10-30 eV range.

Figure 1 shows our R-matrix results and the SMCPP of da Costa *et al.*[17]. Both CC

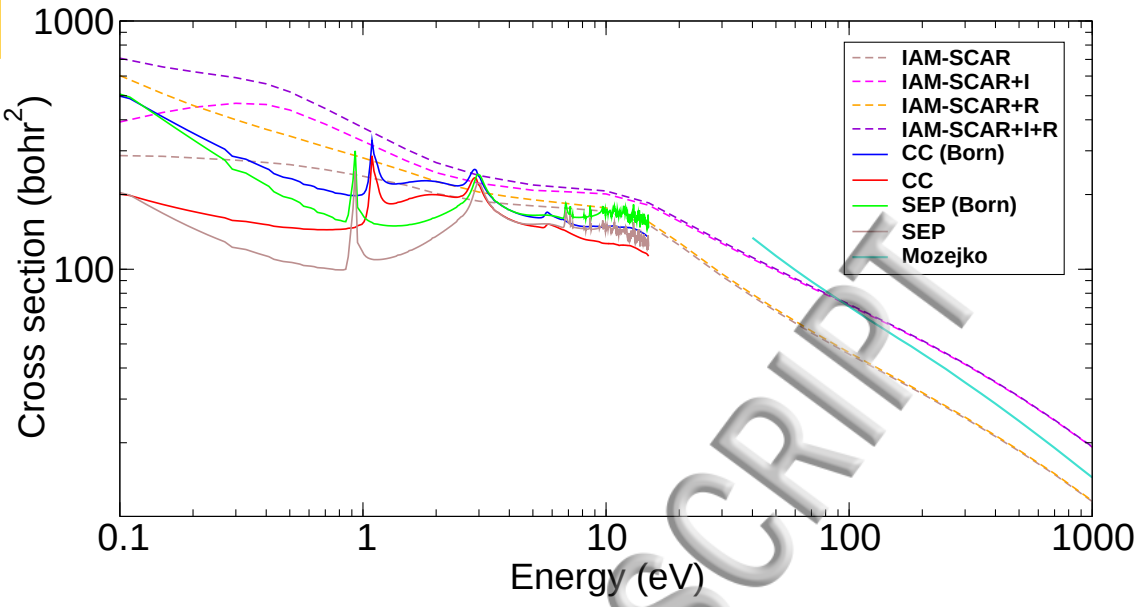

FIG. 2. Integral elastic cross section for electron scattering from thiophene. The IAM-SCAR+R results include rotational excitations; the IAM-SCAR+I ones includes the interference term and the IAM-SCAR+I+R includes both (see text for more details). We also show the 'plain' IAM-SCAR results. The SEP and CC R-matrix results are presented with and without the Born correction as indicated. Also included are the results from Mozejko *et al.*[16].

and SEP approximations produce cross sections with similar profiles, particularly when the Born correction is included. This correction is bigger at lower energies, where the influence of the dipole moment on the collision is stronger. Above the second visible resonance, the size and shape of our R-matrix cross sections are almost identical, except for a well-known feature: our SEP results suffer from the presence of non-physical pseudoresonances, appearing as very narrow peaks in the cross section above ∼6-7 eV. The physical resonances present in thiophene have been discussed elsewhere[19]. Below the second visible resonance, the difference between SEP and CC results is noticeable and we attribute it to a different description of the polarization effect (this difference also leads to slightly different resonance positions). The results from da Costa *et al.*[17] plotted in the figure correspond to their SEP cross section and do not include any correction to incorporate the effect of those partial waves not included in the SMCPP calculation. Agreement with our uncorrected SEP cross sections is excellent, except below 1 eV where our calculation accounts for more of the dipole effect.

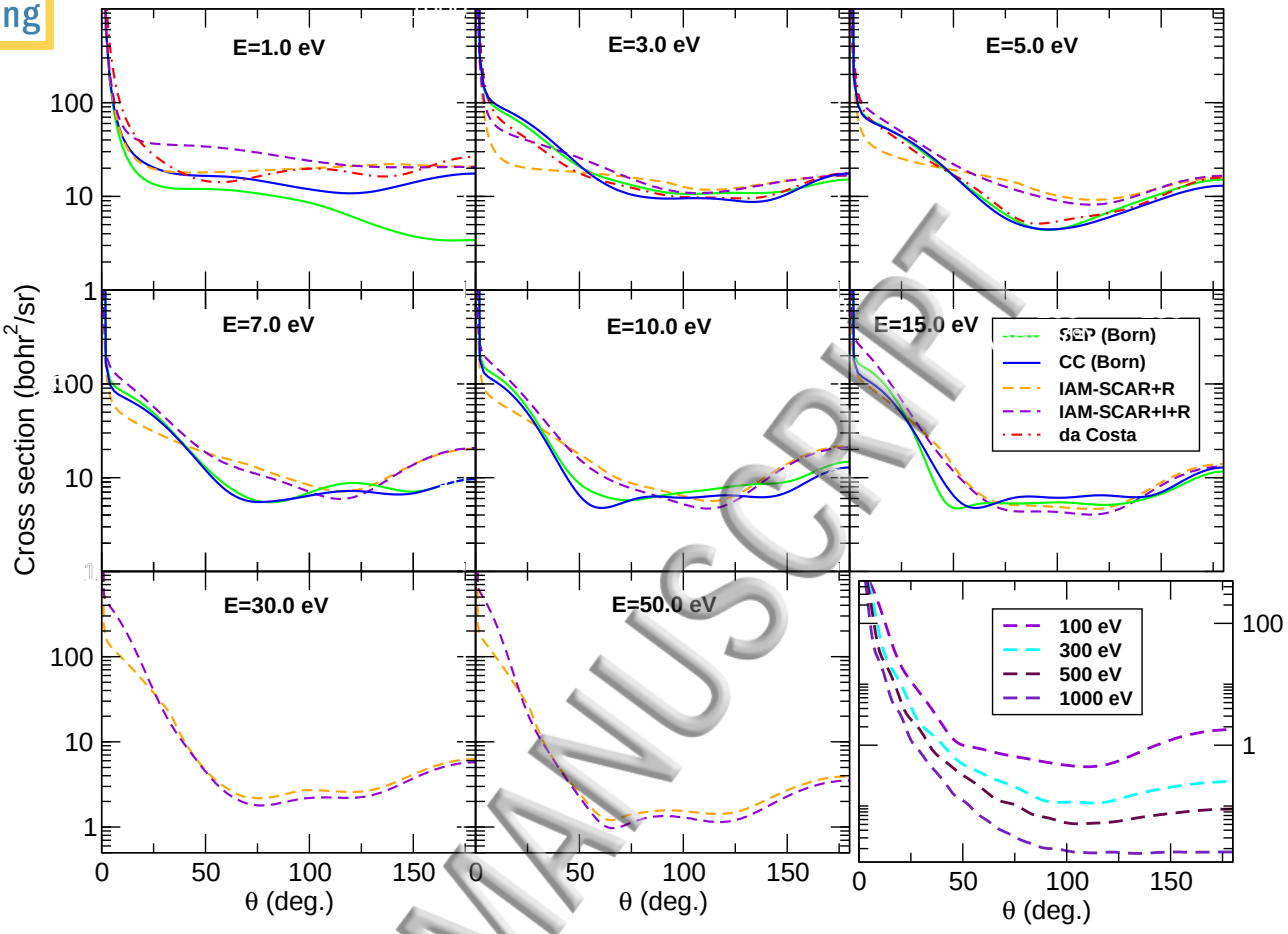

FIG. 3. Elastic differential cross sections for electron scattering from thiophene for the energies indicated in the panels. The R-matrix DCS are Born corrected and are presented up to 15 eV. The IAM-SCAR+I+R DCS are presented for the whole energy range while the IAM-SCAR+R are not shown above 50 eV. Also plotted for 1, 3 and 5 eV are the SMCPP SEP cross sections of da Costa *et al.*[17], this time incorporating a Born based correction. The bottom right hand panel presents IAM-SCAR+I+R DCS for several energies. Note that for this panel the scale for the cross sections is indicated on the right.

In Figure 2, we show the integral elastic cross section for the whole energy range. Four types of results calculated with the IAM-SCAR approach are plotted: 'plain' IAM-SCAR results, IAM-SCAR with the interference term (IAM-SCAR+I), IAM-SCAR including rotations (IAM-SCAR+R) and IAM-SCAR with interference term and including rotations (IAM-SCAR+I+R). It is clearly observable that it is the interference term that makes the bigger difference to the cross section, except for very low energies; above ∼10 eV, the effect

of including the rotational excitation is negligible. All four IAM-SCAR cross sections are, in general, higher than the R-matrix ones, specially those including the interference term, as can be seen in the figure. The best agreement in the energy range where they overlap is between the Born-corrected SEP R-matrix results and the IAM-SCAR ones that don't include the interference term. However, for the IAM model, initially based on single atom scattering processes, the most physically sound representation is that including screening corrections, interference terms and additionally incorporating dipole-rotation interactions, i. e. the IAM-SCAR+I+R calculation. From the R-matrix point of view, starting from a molecular description of the target, the most complete representation corresponds to the CC calculation that includes the Born correction. So despite the better agreement between IAM-SCAR/IAM-SCAR+R calculations and the SEP R-matrix ones at 10 eV, physical considerations lead us to recommend a smooth interpolation between the IAM-SCAR+I+R and the Born-corrected CC data.

Also plotted in Figure 2 are the elastic cross sections obtained by Mozejko *et al.*[16]. As expected, their results are in reasonably good agreement with all our IAM-SCAR data for increasing energies but tending to overestimate the present results for energies below 100 eV, where the IAM representation fails.[32,33]

Figure 3 shows elastic differential cross sections: both SEP and CC R-matrix results (including the Born correction) together with IAM-SCAR+R and IAM-SCAR+I+R DCS are presented for the lower energies as well as the SMCPP results of da Costa *et al.*[17]. Only IAM-SCAR+R (up to 50 eV) and IAM-SCAR+I+R (up to 1000 eV) results are presented for energies above 30 eV.

The shape and size of the R-matrix DCS obtained with both approximations are very similar, with the bigger difference showing at 1 eV. Agreement of these results with da Costa *et al.* is very good at 3 and 5 eV, as was also the case, for example, for pyridine[28]. For 1 eV, however, both the shape and size of the DCS are very different. This discrepancy for 1 eV was also observed for pyrimidine when compared with Schwinger Multichannel results from Winstead and McKoy[46], but in that case it was the R-matrix method that produced bigger cross sections for the higher angles, in poorer agreement with experiment. For these angles, our DCS at 1 eV seems to be more similar in shape to the SE results from da Costa *et al.*[17], a sign that perhaps our calculations underestimate somewhat the polarization effects.

The IAM-SCAR+R and IAM-SCAR+I+R results display visible differences for all ener-

gies for which they are plotted: the effect of the inclusion of the interference term is particularly obvious at small angles. As expected, the IAM-SCAR+R and IAM-SCAR+I+R DCS are very different to the R-matrix ones at low energies. Above 10 eV both methods seem to provide DCS of a similar size, reaching the best agreement at 15 eV, where the shape of the DCS is also very similar.

Looking at the IAM-SCAR+R and IAM-SCAR+I+R DCS for 10 and 15 eV, it is not entirely evident that the IAM-SCAR+R approach will produce integral elastic cross sections closer to the R-matrix ones, as evidenced in Figure 2. In particular, at 15 eV the R-matrix DCS for angles below 25° are between the IAM-SCAR+R and IAM-SCAR+I+R results. However, the integral R-matrix cross sections for this energy are below both the IAM-SCAR+R and IAM-SCAR+I+R ones. This apparent discrepancy can be explained by the fact that the integral elastic cross section, $\sigma^{\text{elastic}}_{\text{molec}}$, corresponds to the following integration of the DCS, $\frac{d\sigma}{d\Omega}(E,\theta)$:

$$\sigma^{\text{elastic}}_{\text{molec}}(E) = 2\pi \int_0^{\pi} \frac{d\sigma}{d\theta}(E,\theta)\sin(\theta)d\theta \tag{5}$$

It is the smaller contribution of the intermediate angles (25° to 70°), where both R-matrix models produce smaller DCS that makes the corresponding integral cross section smaller. The clear difference in size of the integral IAM-SCAR+R and IAM-SCAR+I+R cross section does come from the DCS below 25°. Therefore, the better agreement of the IAM-SCAR+R integral cross section with the R-matrix data seems to be due to a compensation of contributions: the smaller contribution of the very small angles balances the larger contribution of the intermediate angle DCS to give an integrated result that is closer to the R-matrix one.

As stated earlier, we have used a combination of R-matrix and IAM-SCAR approaches in the past to determine cross sections for other targets; however, no interference terms were used for those systems. In the case of pyridine[28], for example, the R-matrix integral elastic cross sections at 10 eV lie between those determined with the IAM-SCAR and IAM-SCAR+R approaches. The agreement of the DCS at this energy was similar to that for thiophene for most of the angular range: the better agreement of the integrated value was probably due to the fact that both methods produce a similar value for the DCS at very small angles, where the dipole effect dominates; pyridine has a much bigger dipole moment than thiophene ($\simeq$2.19 Debye). In the case of pyrazine[26], a non-polar molecule, the agreement of

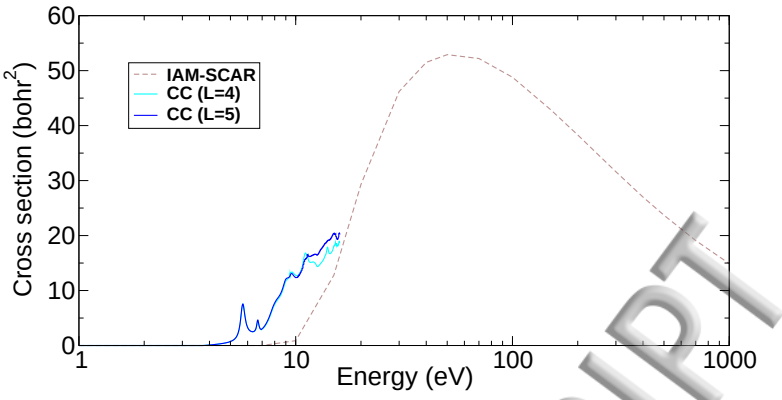

FIG. 4. Integral electronically inelastic cross section for electron scattering from thiophene calculated using the R-matrix and IAM-SCAR methods. R-matrix cross sections from calculations including partial waves up to $l = 4$ and $l = 5$ are plotted.

the DCS at 10 eV was much poorer than for thiophene, as was also the case for 15 eV. For that target, the R-matrix method provided better agreement with experiments and prior theoretical results. In the case of the integral elastic cross section, the IAM-SCAR method produced higher cross sections as is the case for thiophene. This would seem to imply that agreement between R-matrix and IAM-SCAR results in the energy range where both are applied is in general better for targets with a bigger dipole moment.

In Figure 4 we present the total electronically inelastic cross sections obtained with both methods used in this work. The R-matrix results are obtained summing over all 25 states included in the calculation. The figure presents results using partial waves up to $l = 4$ and $l = 5$ to show that the additional partial wave increases the size of the cross section by 10% at the most. Only the IAM-SCAR result is shown, as the interference term does not affect any of the inelastic processes. Note that for this method, the cross section is zero below 7 eV, because the states lying below this threshold are neglected. The first experimental excitation threshold is below 4 eV so the R-matrix cross section is non-zero between 4 and 7 eV. The agreement at 15 eV is, however, good and an interpolation between the R-matrix and the IAM-SCAR results could be easily done.

Finally, for completeness, we present in Figure 5 the total integral cross sections. In the case of the R-matrix data this corresponds to the sum of the Born corrected elastic cross section and the total inelastic cross section. In the case of the higher-energy method we present results obtained with the IAM-SCAR, IAM-SCAR+R and IAM-SCAR+I ap-

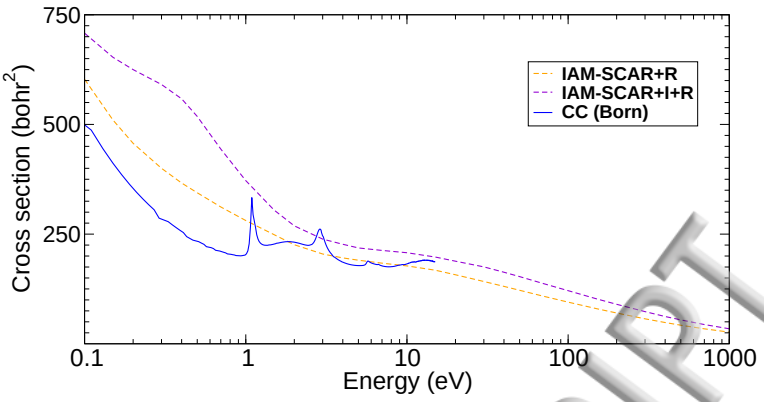

FIG. 5. Total cross sections for electron scattering from thiophene. The R-matrix results are calculated at the CC level and include the Born correction for the elastic contribution; two versions of the IAM-SCAR method, IAM-SCAR+R and IAM-SCAR+I+R are presented.

proaches. Similarly to the elastic integral cross sections, the best agreement is found with the IAM-SCAR method, i.e., when no interference terms is added.

V. CONCLUSIONS

We report elastic and inelastic cross sections for electron scattering from thiophene in the energy range 0.1-1000 eV, determined using the R-matrix and the IAM-SCAR methods at lower and higher energies respectively. Therefore, we provide for the first time a full set of cross sections in a fairly broad energy range. Despite the better agreement at 15 eV between the Born corrected SEP R-matrix results and the IAM-SCAR results without interference terms, we recommend use of the Born-corrected CC results for low energies and the IAM-SCAR+I+R for high energies, as these are obtained using the more physically accurate approaches. Agreement with prior SMCPP results at lower energy[17] and those obtained using the additivity rule at higher energy[16] is good.

The agreement between R-matrix and several IAM-SCAR integral elastic cross sections is reasonably good and similar to that obtained for pyrazine[26]: a smooth interpolation between the R-matrix data at 10 eV and the IAM-SCAR+I+R data at 30 eV can be envisaged. This combination of methods has proven once more to be suitable in providing cross sections for a broad energy range, as shown in the past for other targets.[26–28]

The question remains open, however, as to the better agreement of the R-matrix integral

elastic cross sections with the IAM-SCAR and IAM-SCAR+R results, i.e. those that do not include the interference terms: it is clear from the comparison of DCS that at 10 eV the IAM-SCAR+I+R method produces results in better agreement with the R-matrix results for small angles; this is less obvious for 15 eV. However, we note that the use of a Born correction and the R-matrix method does not describe the DCS at very small angles particularly accurately (see, for example, the discussion provided by Regeta *et al.*[13]); for molecules with a bigger dipole moment (e.g. pyrimidine) we expect it to overestimate the DCS in this angular range. Since differences between IAM-SCAR DCS calculated with and without the interference term are mainly due to the small scattering angles, experimental validation of the results would require extremely precise experimental conditions as far as the angular resolution is concerned.

VI. ACKNOWLEDGMENTS

We are grateful to Dr. Romarly da Costa for providing us the numerical data for the SMCPP cross sections. This work was supported by Fundação para a Ciência e a Tecnologia (FCT-MCTES), Radiation Biology and Biophysics Doctoral Training Programme (RaBBiT, PD/00193/2012); UID/Multi/04378/2013 (UCIBIO); UID/FIS/00068/2013 (CEFITEC); and scholarship grant number SFRH/BD/106031/2015 to A Loupas. JDG was supported by EPSRC grant EP/P022146/1. F.B. and G.G. acknowledge partial financial support from the Spanish Ministry MINECO (Project FIS2016-80440). A.I.L. is registered on the doctoral of the UNED university.

REFERENCES

[1]P. Čarsky and R.Čurík, *Low-Energy Electron Scattering from Molecules, Biomolecules and Surfaces* (CRC Press: Boca Raton, 2011).

[2]M. Bug, W. Baek, H. Rabus, C. Villagrasa, S. Meylan, and A. Rosenfeld, Rad. Phys. Chem. **130**, 459 (2017).

[3]L. Alves, P. Coche, M. Ridenti, and V. Guerra, Eur. Phys. J. D **70(6)** (2016).

[4]R. White, M. Brunger, N. Garland, R. Robson, K. Ness, G. García, J. de Urquijo, S. Dujko, and Z. Petrovíc, Eur. Phys. J. D **68:125** (2014).

[5]B. Boudaïffa, P. Cloutier, D. Hunting, M. A. Huels, and L. Sanche, Science **287**, 1658 (2000).

[6]I. Baccarelli, I. Bald, F. A. Gianturco, E. Illenberger, and J. Kopyra, Phys. Rep. **508**, 1 (2011).

[7]J. Gorfinkiel and S. Ptasinska, J. Phys. B **50**, 182001 (2017).

[8]D. Bouchiha, J. Gorfinkiel, L. Caron, and L. Sanche, J. Phys. B: At., Mol. Opt. Phys. **39**, 975 (2006).

[9]C. Trevisan, A. Orel, and T. Rescigno, J. Phys. B: At., Mol. Opt. Phys. **39**, L255 (2006).

[10]S. Tonzani and C. Greene, J. Chem. Phys. **125**, 094504 (2006).

[11]M. Fuss, A. M. noz, J. Oller, F. Blanco, D. Almeida, P. L. ao Vieira, T. Do, M. Brunger, and G. García, Phys. Rev. A: At., Mol. Opt. Phys. **80**, 052709 (2009).

[12]A. Gauf, L. Hargreaves, A. Jo, J. Tanner, M. Khakoo, T. Walls, C. Winstead, and V. McKoy, Phys. Rev. A: At., Mol. Opt. Phys. **85**, 052717 (2012).

[13]K. Regeta, M. Allan, Z. Mašín, and J. Gorfinkiel, J. Chem. Phys. **144**, 024302 (2016).

[14]Z. Mašín, J. Gorfinkiel, D. Jones, S. Bellm, and M. Brunger, J. Chem. Phys. **136**, 144310 (2012).

[15]D. Gramec, L. Peterlin, and M. Sollner, Chem. Res. Toxicol. **8**, 1344 (2014).

[16]P. Mozejko, E. Ptasinska-Denga, and C. Szmytkowski, Eur. Phys. J. D **66**, 20659 (2012).

[17]R. da Costa, M. do N. Varella, M. Lima, and M. Bettega, J. Chem. Phys. **138**, 194306 (2013).

[18]M. Vinodkumar, H. Desai, and P. Vinodkumar, RSC Adv. **5**, 24564 (2015).

[19]A. Loupas, K. Regeta, M. Allan, and J. D. Gorfinkiel, The Journal of Physical Chemistry A **122**, 1146 (2018), https://doi.org/10.1021/acs.jpca.7b11865.

[20]K.R.Asmis, Ph.D. thesis, Université de Fribourg, Switzerland (1996).

[21]A. Modelli and P. Burrow, J. Chem. Phys. A **108**, 5721 (2004).

[22]M. N. Hedhili, P. Cloutier, A. D. Bass, T. E. Madey, and L. Sanche, J. Chem. Phys. **125**, 094704 (2006).

[23]M. V. Muftakhov, N. Asfandiarov, and V. I. Khvostenko, J. Electron. Spectrosc. Relat. Phenom. **69**, 165 (1994).

[24]D. Raj, Phys. Lett. **160**, 571 (1991).

[25]K. Joshipura and P. Patel, Z. Phys. D **29**, 269273 (1994).

[26]A. Sanz, M. Fuss, F. Blanco, J. Gorfinkiel, D. Almeida, F. da Silva, P. L. ao Vieira, M. Brunger, and G. García, J. Chem. Phys. **139(18)**, 184310 (2013).

[27]A. Sanz, M. Fuss, F. Blanco, Z. Mašín, J. Gorfinkiel, F. Carelli, F. Sebastianelli, F. Gianturco, and G. García, Appl. Radiat. Isot. **83-Part B**, 57 (2014).

[28]A. Sieradzka, F. Blanco, M. Fuss, Z. Mašín, J. Gorfinkiel, and G. García, J. Phys. Chem. A **118**, 6657 (2014).

[29]J. Tennyson, Phys. Rep. **491**, 29 (2010).

[30]A. Dubuis, A. Verkhovtsev, L. Ellis-Gibbings, K. Krupa, F. Blanco, D. Jones, and M. Brunger, J. Chem. Phys. **147**, 054301 (2017).

[31]F. Blanco, L. Ellis-Gibbings, and G. García, Chemical Physics Letters **645**, 71 (2016).

[32]F. Blanco and G. García, Phys. Rev. A **67**, 022701 (2003).

[33]F. Blanco and G. García, Phys. Lett. A **317**, 458 (2003).

[34]P. G. Burke, *R-Matrix Theory of Atomic Collisions: Application to Atomic, Molecular and Optical Processes* (Springer, 2011).

[35]J. M. Carr, P. G. Galiatsatos, J. D. Gorfinkiel, A. G. Harvey, M. A. Lysaght, D. Madden, Z. Mašín, M. Plummer, J. Tennyson, and H. N. Varambhia, Eur. Phys. J. D **66**, 20653 (2012).

[36]Z. Mašín and J. D. Gorfinkiel, The Journal of Chemical Physics **135**, 144308 (2011).

[37]N. Sanna and F. Gianturco, Comput. Phys. Commun. **114**, 142 (1998).

[38]F. Gianturco and A. Jain, Phys. Rep. **143**, 347 (1986).

[39]M. H. Palmer, I. C. Walker, and M. F. Guest, Chem. Phys. **241**, 275 (1999).

[40]H. Haberkern, K. Asmis, M. Allan, and P. Swiderek, Phys. Chem. Chem. Phys. **5**, 827 (2003).

[41]W. Flicker, O. Mosher, and A. Kupperman, J. Chem. Phys. **64**, 1315 (1976).

[42]R. D. J. I. Editor, "Nist standard reference database," `http://http://cccbdb.nist.gov`, accessed: 2017-10-04.

[43]A. McClellan, *Tables of experimental dipole moments* (W.H.Freeman, 1963).

[44]M. Gussoni, R. Rui, and G. Zerbi, J. Mol. Struct. **447**, 163 (1998).

[45]H.-J. Werner, P. J. Knowles, G. Knizia, F. R. Manby, M. Schütz, P. Celani, W. Györffy, D. Kats, T. Korona, R. Lindh, A. Mitrushenkov, G. Rauhut, K. R. Shamasundar, T. B. Adler, R. D. Amos, A. Bernhardsson, A. Berning, D. L. Cooper, M. J. O. Deegan, A. J. Dobbyn, F. Eckert, E. Goll, C. Hampel, A. Hesselmann, G. Hetzer, T. Hrenar, G. Jansen,

C. Köppl, Y. Liu, A. W. Lloyd, R. A. Mata, A. J. May, S. J. McNicholas, W. Meyer, M. E. Mura, A. Nicklass, D. P. O'Neill, P. Palmieri, D. Peng, K. Pflüger, R. Pitzer, M. Reiher, T. Shiozaki, H. Stoll, A. J. Stone, R. Tarroni, T. Thorsteinsson, and M. Wang, "Molpro, version 2015.1, a package of ab initio programs," (2015), see http://www.molpro.net.

[46]K. Regeta, M. Allan, C. Winstead, V. McKoy, Z. Mašín, and J. D. Gorfinkiel, J. Chem. Phys. **144**, 024301 (2016).